Latin American Journal of Solids and Structures
www.lajss.org

Structural Health Monitoring of Sandwich Structures Based on Dynamic Analysis

Abstract

This work aims to contribute to the development of SHM systems based on vibration methods to be applied on sandwich structures. The main objective is focused on experimental damage identification via changes in the Frequency Response Function (FRF) with the usage of damage metrics. Specimens of sandwich structures made from skins of epoxy resin reinforced by glass fiber and a core of PVC foam are manufactured. First, preliminary non-damped Finite Element (FE) models are performed, and results obtained are used to define the frequency range of interest for the experimental procedure. After that, vibration experimental analyses are carried out on undamaged specimens. The natural frequencies are compared to the preliminary FE results. Second, experimental analyses are performed on damaged specimens with and without piezoelectric sensors. Then, damage metric values are calculated based on FRFs for damaged and undamaged structures, which were obtained from experimental and FE analyses (with damping effects). In addition, a new procedure is proposed to improve the quality of results provided by the damage metric. It is shown that the new procedure is very effective to identify the damage using both amplitude and phase from FRFs. Lastly, it is discussed the potential and limitations of the FE model to predict damage metric values, comparing to experimental data.

Keywords

Structural Health Monitoring, Sandwich Structures, Vibration Methods, Finite Element Analysis, Experimental Analysis.

Denys Marques[a]
Felipe R. Flor[a]
Ricardo de Medeiros[b]
Carlos do Carmo Pagani Junior[c]
Volnei Tita[a*]

[a] Departamento de Engenharia Aeronáutica, São Carlos, Universidade de São Paulo (USP), São Carlos, SP, Brasil. E-mail: adenys.marques@usp.br, feliperendeiro88@gmail.com, voltita@sc.usp.br

[b] Departamento de Engenharia Mecânica, Colégio de Ciências Tecnológicas, Universidade Estadual de Santa Catarina - Udesc, Joinville, SC, Brasil. E-mail: ricardo.medeiros@udesc.br

[c] Universidade Estadual de São Paulo (UNESP), São João da Boa Vista, SP, Brasil. E-mail: paganni.carlos@gmail.com

*Corresponding author:

http://dx.doi.org/10.1590/1679-78254309

Received: July 24, 2017
In Revised Form: November 17, 2017
Accepted: February 07, 2018
Available online: March 19, 2018

1 INTRODUCTION

Composite sandwich structures consist of two outer layers (skins) generally thinner and made of a rigid material, which surround a core of low stiffness, generally thicker and of lower density (Callister and Rethwisch (2012)). The resulting structure has low density, high flexural stiffness and high sound insulation. These characteristics are very strategic for aeronautical industry (Nguyen et al. (2005); Leijten et al. (2009); Pourmoayed et al. (2017)). Concomitantly with the increase in its use, it is necessary to develop methods for monitoring its structural integrity due to the complex process to predict damage in sandwich structures. And, the starting point of any Structural Health Monitoring system (SHM) is the initial damage detection. For this purpose, one of the most used methods is based on the vibration response of the structures due to easy implementation and low cost. In addition, vibration based method presents no requirement for visual inspection, "automation" capability, "global" coverage (in the sense of covering large areas of the structure), and capability of working at a "system level".

The physical principle for a SHM system based on vibration analysis is that modal parameters such as natural frequencies, vibration modes or damping factors are functions of the structural properties (integrity, strength, rigidity, damping, etc.). Therefore, changes in these structural parameters resulting from structural damage (such as delaminations, cracks, etc.) would reflect as a change in modal parameters (Doebling et al. (1996)).

It can be found in the literature some examples of successful application of this principle to estimate and locate damage in sandwich and composite structures (Yam et al. (2003); Oruganti et al. (2009); Luchinsky et al. (2011); Medeiros et al. (2017)). Lestari and Qiao (2005) used smart sensors to perform damage detection, location and quantification of damage based on curvature mode shapes. The authors used honeycomb sandwich beams made of

glass fibers and polyester resin with the core consisting of corrugated cells damaged and undamaged. Amir et al. (2010) used the dynamic response of a honeycomb sandwich structure to detect multi-site damage. The authors determined variation of natural frequencies and damping ratios to estimate the damage. The studies concluded that change in damping ratio was another way to detect damage. The researchers also discussed how low velocity impact damage, such as dropped tools during maintenance, can cause small indentations in the structure. They highlighted that the use only of natural frequencies for detecting damage cannot be reliable for identifying initial damages on the structures. Thus, for composite structures, the interest by the academy over the use of modal damping variation has increased since this criterion is very sensible to damage. Therefore, the determination of the FRF (Frequency Response Function) is a kind of approach in this context. For example, Dhamande and Bhaskar (2014) made use of the first three natural frequencies and mode shapes to detect and localize two types of damage - debonding and core crushing - in honeycomb sandwich beams, which had core in aluminum and skins in carbon fiber reinforced plastic. Li et al. (2015) investigated the use of vibration characteristics to monitor the integrity of composite lattice truss sandwich structures. The authors pointed out that, despite the increasing number of studies investigating this type of structure, the literature is still insipient in non-destructive evaluation techniques and structural health monitoring applied to these components. They verified that local deformation in vibration modes and the decrease of natural frequency occur only when the damage is large, demonstrating the need of damage metrics. Numerical and experimental analyses were then performed to investigate a new damage index proposed by the authors, which demonstrated its applicability and reliability in damage localization. Idriss et al. (2015) compared the responses of a sandwich beam made of glass fiber laminates and PVC foam core to linear and nonlinear vibration. They performed experimental analyses for different lengths of debonding damage and verified that nonlinear parameters appear to be more sensitive in the evaluation of damage. Mustapha et al. (2016) used ultrasonic guided wave signals to evaluate barely visible indentation damage in beams and panels of carbon fiber composite sandwich with honeycomb core. They investigated two different damage indexes: one based on changes in the characteristics of the guided waves and other based on time-reversal algorithm. Their results showed high sensitivity of the guided waves to identify indentations as small as 0.2 mm. The damage index based on the time-reversal algorithm demonstrated to be less sensitive to damage than the one based on changes in the magnitude of guided waves, but the first one has the advantage of not requiring a reference as the state prior to damage.

Considering the scenario pointed above, this work aims to contribute to the development of SHM systems based on vibration methods to be applied on sandwich structures. The main objective is focused on the damage identification. Specimens of sandwich structures made of skins in epoxy resin reinforced by glass fiber and a core of PVC foam are manufactured. First, preliminary finite element models (without damping effects) are developed in order to analyze the dynamic characteristics of undamaged and damaged structures with presence or not of two piezoelectric sensors. Then, vibration experimental analyses are performed on undamaged specimens of sandwich structures based on finite element results. The mode shapes and natural frequencies are compared to the preliminary computational results. Second, vibration experimental analyses are carried out on undamaged and damaged specimens of sandwich structures with and without piezoelectric sensors. After that, damage metrics are calculated based on Frequency Response Functions, which were obtained from experimental analyses and finite element models (with damping effects). In addition, this work brings a new procedure in order to improve the quality of results provided by the damage metric proposed by Mickens et al. (2003).

2 MATERIALS AND METHODS

2.1 Sandwich structures specimens: Materials and sensors

The sandwich structures were made from glass fiber/epoxy resin skins and PVC foam core. The specimens have three output regions, one input point (position 1) and one damage area. The dimensions for the specimens are shown in Figure 1. As noted in the schematics, the positions 2 and 3 have accelerometers or Macro Fiber Composite (MFC) piezoelectric sensors. Position 4 is the area of damage (debonding), which was obtained by replacing the adhesive component by a Teflon™ layer through the overlap area. Position 5 has always an accelerometer, which is considered as a reference point.

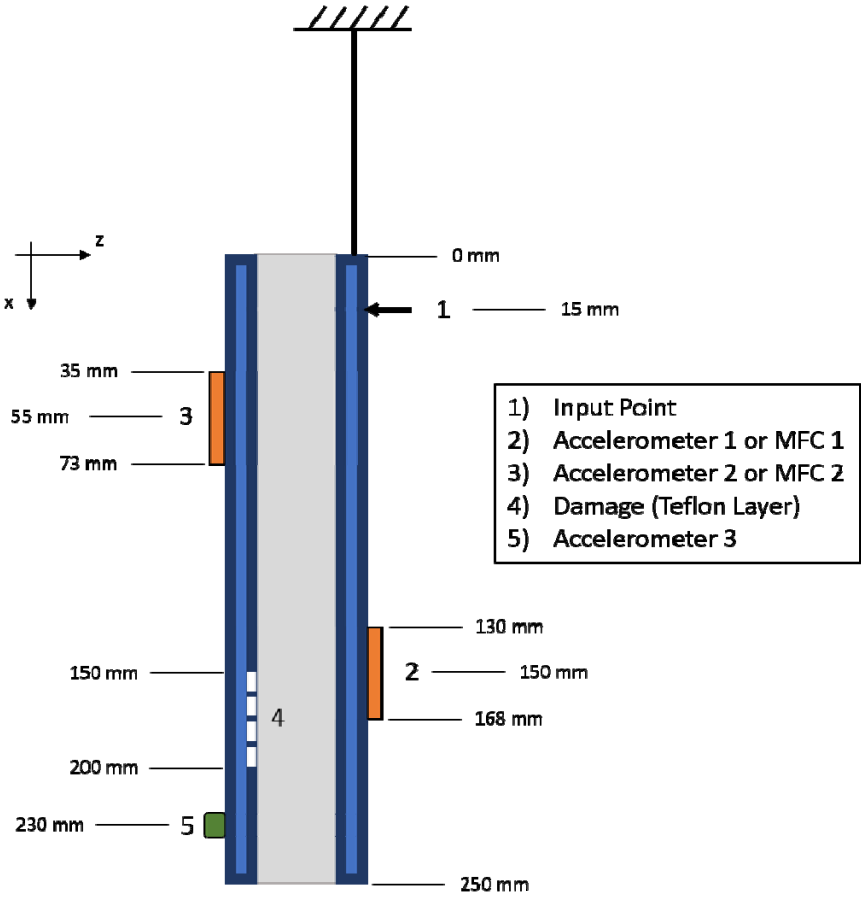

Figure 1: *Schematic representation of the sandwich structure specimens.*

The skins were made from unidirectional glass fibers and epoxy Araldite LY 1564 BR resin catalyzed by REN HY 150 BR. The plies were stacked as $[0°/+45°/-45°]_S$ configuration. The laminated plates were manufactured at Laboratory of Aeronautic Structures (University of São Paulo). They were produced by laying up dry fibers on top of a flat glass mold in accordance to the stacking sequence. The resin was applied using vacuum system and it was cured under 25ºC for 12 hours. The mechanical properties of the skins were not obtained experimentally, for that reason, values used in the computational analyses were found in the literature (Singh and Talreja (2010)). These values are shown in Table 1.

Table 1: *Elastic properties of skin (from Singh and Talreja, 2010).*

Properties	Unit	Value
E_{11}	GPa	44.80
E_{22}	GPa	11.30
E_{33}	GPa	11.30
G_{13}	GPa	4.86
G_{23}	GPa	4.45
G_{12}	GPa	4.86
ν_{12}	-	0.28
ν_{13}	-	0.28
ν_{23}	-	0.28
ρ	kg/m^3	1580

The core was made of PVC foam H60 from Divinicell, which is commonly used by the aeronautical industry. In fact, the elastic properties and strength values under tension and compression were determined by Tita and Caliri Junior (2012); Caliri Junior et al. (2012) and Tita et al. (2012). These values are shown in Table 2.

The piezoelectric sensor for monitoring the sandwich structure was MFC (Macro Fiber Composite) – M2814 by Smart Material Corp., which uses d_{33} mode of piezoelectricity. This sensor was chosen because it offers high performance, flexibility (mainly for structures under flexural loads like aircraft panels) and reliability in a cost competitive device. Moreover, because MFC is more sensitive than AFC (Active Fiber Composite) sensors, they are easy to assembly on the structure and to use ("plug and play"). The piezoelectric sensor coefficients of constitutive matrix were obtained by Sartorato et al. (2015) and Medeiros (2016), which are shown in Table 3.

The skins were jointed to the core by using the same epoxy resin to manufacture the laminated plates. This bonding process was performed inside an oven at 65ºC for 8 hours. The sandwich plate was carefully cut into specimens of sandwich beams with dimensions about 250 mm of length, 25 mm of width and 12 mm of thickness. To create a debonding damage, a Teflon™ layer was introduced during the bonding process as shown by the Figure 1. Therefore, damaged and undamaged specimens were investigated with and without piezoelectric sensors. Finally, the specimens analyzed are identified in accordance to the following code:

- S1: Intact (undamaged) specimen
- S2: Damaged specimen
- E0P0: Absence of MFC (Output by: "A1", "A2", "A3")
- E0P1: Presence of one MFC (Output by: "P1", "A2", "A3")
- E0P2: Presence of two MFCs (Output by: "P1", "P2", "A3")

where "A" corresponds to accelerometer and "P" corresponds to MFC sensor. Besides, "1" is related to the position 2 (Fig. 1), "2" is related to the position 3 (Fig. 1) and "3" is related to the position 5 (Fig. 1). For example, specimen S1E0P1 means an undamaged sandwich structure with one MFC. Then, the output results can be obtained from the MFC sensor at position 2 ("P1") and/or from the accelerometer at position 3 ("P2") and/or from the accelerometer at position 5 ("A3").

Table 2: *Elastic properties of PVC foam core (from Tita and Caliri Junior (2012); Caliri Junior et al. (2012) and Tita et al. (2012)).*

Properties	Unit	Value
E_{11}	GPa	0.034
E_{22}	GPa	0.034
E_{33}	GPa	0.112
G_{13}	GPa	0.02
G_{23}	GPa	0.02
G_{12}	GPa	0.0139
ν_{12}	-	0.22
ν_{21}	-	0.22
ν_{13}	-	0.35
ν_{31}	-	0.11
ν_{23}	-	0.35
ν_{32}	-	0.11
ρ	Kg/m^3	60.00

Table 3: *Coefficients of constitutive matrix for piezoelectric sensor (M2814) (from Sartorato et al. (2015) and Medeiros (2016)).*

Properties	Unit	Value
C_{11}	GPa	1.47
C_{12}	GPa	1.19
C_{13}	GPa	1.22
C_{33}	GPa	59.70
C_{44}	GPa	23.20
C_{66}	GPa	0.28
e_{13}	C/m^2	-0.05
e_{15}	C/m^2	0.17
e_{33}	C/m^2	21.07
ϵ_{11}	nF/m	0.62
ϵ_{33}	nF/m	15.40
ρ	Kg/m^3	5440

2.2 Experimental set-ups and instrumentation

The vibration tests were limited to the free-free boundary condition. In order to achieve this, the specimens were connected to a metal structure support via a thin wire. The data was acquired using LMS SCADAS Mobile, which was set to cover a bandwidth of 4096 Hz with 8193 spectral lines. The apparatus was set to compute the mean values out of 5 repetitions to reduce random fluctuations or noise. Also, only data with reasonable high coherence values for the range of interest was used. Besides, for the piezoelectric sensor previously mentioned, data acquisition was also performed using three accelerometers Piezotronics Model 352C22, which had the sensitivities of 9.57 mV/g, 9.31 mV/g and 9.96 mV/g. The input load was performed via an impulse force Piezotronics hammer Model PCB 0860C3. Figure 2 shows details about the input point (position 1) and location of accelerometer 1 ("A1" – position 2).

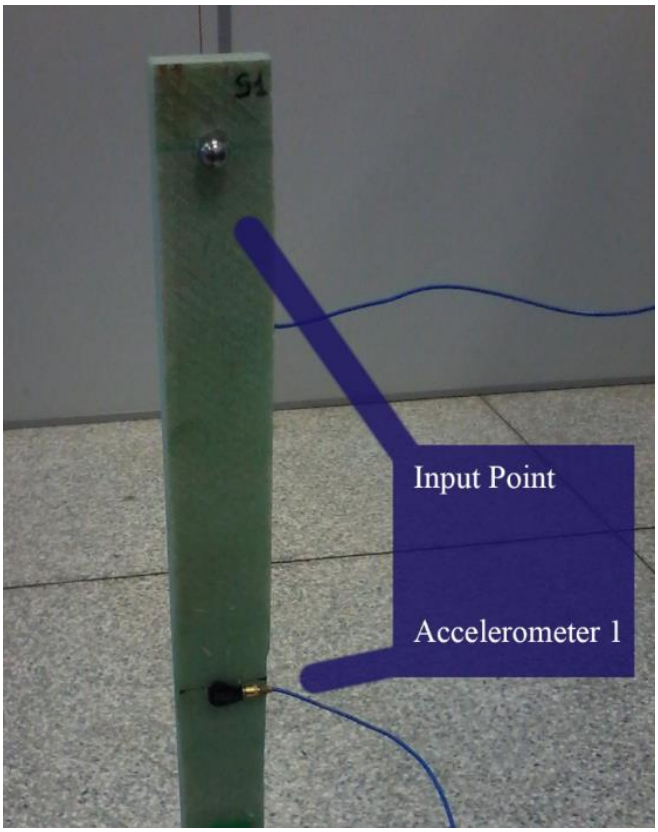

Figure 2: *Details of the experimental set-up for free-free boundary conditions of sandwich structure: input and output points (Flor (2015)).*

2.3 Experimental procedures

The experimental procedures were carried out in 3 sequential steps. The first analyses compared the dynamic response of the specimens S1E0P0, S1E0P1 and S1E0P2 in order to verify the influence of the piezoelectric sensor on the structural behavior. The second ones compared the dynamic response of the specimens S1E0P0 and S2E0P0 in order to verify the influence of the presence of damage in the sandwich structure. The third analyses compared the dynamic response of specimens from MFCs in order to verify the possibility of using their dynamic signature to identify the damage. All comparisons were performed by using damage metrics, as well.

3 DAMAGE METRICS

The damage was quantified by using four different damage metrics. One of the methods used to determine the damage index was proposed by Mickens et al. (2003). This method considers the magnitudes of the FRFs for both the intact (undamaged) and damaged structures. The damage index (DI) can be calculated by the following equations (1) and (2):

$$y(f) = \left| \frac{|H_I| - |H_D|}{|H_I|} \right| \tag{1}$$

$$DI = \frac{1}{f_2 - f_1} \int_{f_1}^{f_2} y(f) df \tag{2}$$

For a discrete sampling, Equation (2) can be rewritten as

$$DI = \frac{\Delta f}{f_2 - f_1}\sum_{i=1}^{n} y_i(f) \tag{3}$$

where H_I and H_D are the FRF amplitudes of undamaged (intact) and damaged structure, respectively, for a certain frequency range $[f_1, f_2]$ and certain frequency increment Δf and n points of the FRF signal. In addition, the damage metric can be also calculated as shown by Equations (4) to (6):

$$\phi_x = \tan^{-1}\left(\frac{\mathrm{Im}(H_x)}{\mathrm{Re}(H_x)}\right); x = I, D \tag{4}$$

$$y(f) = \left|\frac{|\phi_I| - |\phi_D|}{|\phi_I|}\right| \tag{5}$$

$$DI = \frac{\Delta f}{f_2 - f_1}\sum_{i=1}^{n} y_i(f) \tag{6}$$

Where ϕ_I and ϕ_D are the FRF phase angle value of undamaged (intact) and damaged structure, respectively, for a certain frequency range $[f_1, f_2]$ and certain frequency increment Δf, as well.

The damage metric proposed by Mickens is strictly based on the relative differences of magnitude between the dynamic signatures of the intact (undamaged) and damaged specimens. This procedure includes one particular issue. The damage index has a tendentious behavior because of its choice to use the FRF of the intact specimen in the denominator. When H_I approaches zero, the value of $y(f)$ can become unreasonably high, even when the absolute difference between H_I and H_D is small. The same behavior can be also observed when applying Mickens' method into phase data. Figure 3 shows an example from an experimental result where low values of H_I produce a high contribution to damage at a frequency range that has actually no damage.

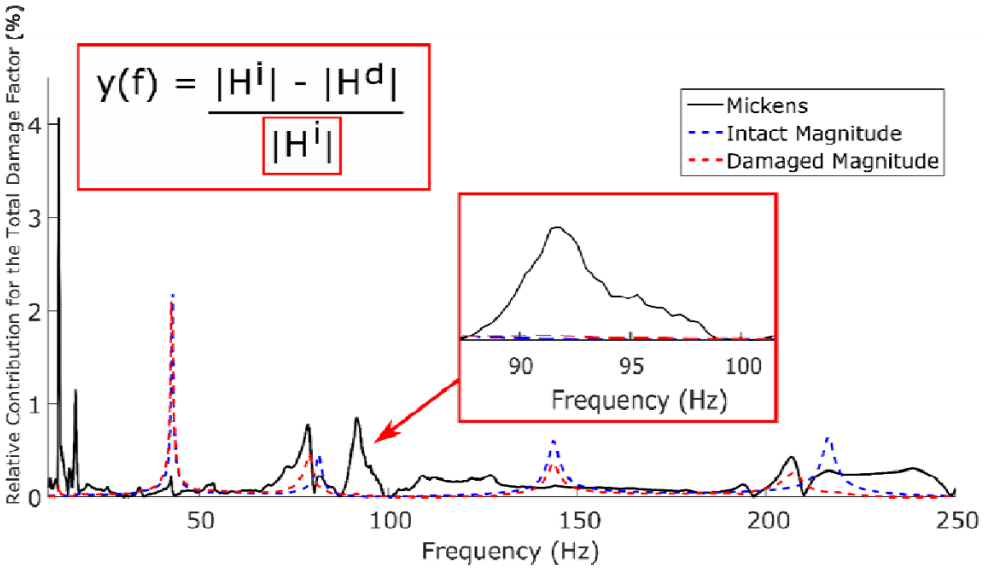

Figure 3: *Mickens' damage metric – Low value divisions.*

3.1 Proposed procedure

To solve the issue pointed above, a procedure was proposed. Thus, two modifications should be implemented into the metric. The first step consists on the implementation of a filter that reduces the occurrences of small denominators in the calculations. This filter operates on both FRFs for the intact (undamaged) and damaged structures. This is achieved by the following procedure:

- The third quartile of the data is automatically accepted as default. To obtain the third quartile, it is necessary to first arrange the values of the array in crescent order. The third quartile corresponds to the value between the median and the highest value of the array. In other words, given an array with *n* elements, if this array is arranged in crescent order, the third quartile will be the value stored at the $0.75 \times n$ elements.
- The values bellow the third quartile are only considered if their magnitude is greater than 15% of the highest value of the data. This step prevents data of reasonable magnitude to be ignored in systems that contain a low standard deviation.
- A range will only be ignored if it has been filtered in both the intact and damaged responses. By the end of the process, the filter can accept a number of values that cover from 25% up to 100% of original data. A value will be only ignored during the damage metric calculation, if it is in a filtered frequency for both intact and damaged FRFs. The overall result of this process is displayed in Figure 4.

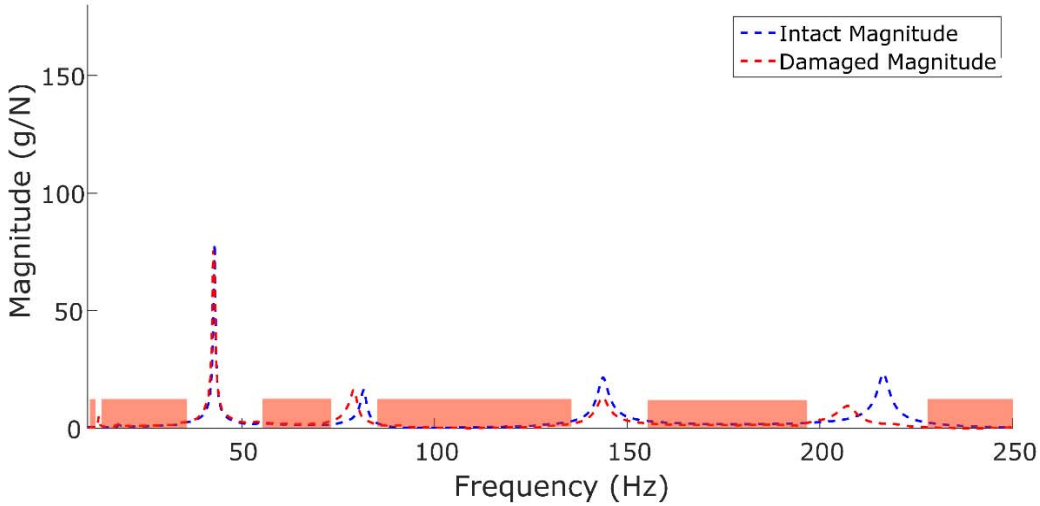

Figure 4: *Filtering of specific frequency ranges of data: Proposed procedure.*

The next step has the purpose of solving the issues with the tendentious behavior of the damage contribution. This is solved by changing the denominator of the Equation (1), using max(H_I, H_D). Thus, the modified damage metric avoids divisions by small numbers, which provide high values for damage metric.

In fact, in the literature, it is possible to find different approaches for calculating damage metrics. In the present work, it was used two more damage metrics in order to compare their results with Mickens' damage metric and the proposed one. In the paper written by Sartorato et al. (2017), it was discussed in detail the potentialities and limitations of different damage metrics, including Mickens' metric. Therefore, based on this publication, it was selected the following metrics:

$$\text{Metric I: } \frac{\sum_{i=1}^{n} \left| H_D(f_i) - H_I(f_i) \right|}{\sum_{i=1}^{n} \left| H_I(f_i) \right|} \tag{7}$$

$$\text{Metric II: } \sum_{j=1}^{n} \frac{\sum_{i=1}^{n} \left| \frac{H_D(f_i) - H_I(f_i)}{H_I(f_i)} \right|}{f_j - f_o} \tag{8}$$

where the magnitude of the amplitude or phase (H_I for undamaged structure and H_D for damaged structure) of the FRFs are used in the calculus, considering a frequency range that includes n points of the FRF signal including different vibration modes. For those metrics, f_o is the lower frequency of the range of interest.

4 FINITE ELEMENT ANALYSIS

The simulations via Finite Element Analysis (FEA) for the sandwich structures were performed using the commercial software package ABAQUS™. The skins were modeled by a total of 600 shell elements S4R (4-nodes shell element), while the core and MFCs sensors were modeled by solid elements. The core was meshed using 2000 C3D8R type elements, which are 8-nodes linear bricks for 3D stress analyses. MFCs were meshed using 660 C3D20RE type elements, which are20-nodes quadratic bricks with mechanical and dielectric degrees of freedom. It is important to highlight that a mesh sensibility analysis was performed in order to verify the influence of the mesh in the modal analyses. The first models were developed by using 2600 elements, which were compared to second ones with more refined mesh (9500 elements). After this investigation, it was observed only very small variation between natural frequencies (less than 2%), showing that it was not required to use more refined mesh.

The adhesive layer between skin and core was simulated by using the "tie" algorithm implemented in ABAQUS™. Hence, the adhesive was considered perfect and not deformable with no thickness. The damage was defined simply as a region without the tie constraint, allowing the surfaces to separate freely. The free-free boundary conditions for the specimen were simulated using the engineering feature "spring" as experimental tests. The stiffness of the "spring" was assumed too low (300 N/m) for avoiding any interference in analyses process. Figure 5 shows specimen S2E0P2 (which contains damage and two MFC sensors).

The dynamic analyses were performed via the "Steady-State Dynamics Modal". This step solution was preceded by the "Frequency" step, which calculates the eigen frequencies for the non-transient condition. The eigenproblem was solved using Lanczos eigensolver, which is implemented in ABAQUS™. After that, the experimental damping factors were considered to improve the numerical models. The damping factors used were obtained by approximating the modal peaks of the experimental FRFs into independent second order transfer functions (peaking method). Therefore, each transfer function had a single natural frequency and a single damping factor associated to it. This procedure was made using Matlab™ and frequency domain identification tools.

It is important to highlight that this FE model was a preliminary computational investigation, and it was developed to provide a prediction of the dynamic behavior for the real structure, aiding the experimental analysis and vice-versa. In fact, non-damped analyses could predict the range of frequencies to be investigated in the experiments, and the damped analyses were carried out to simulate more accurately sandwich structures monitored by smart sensors.

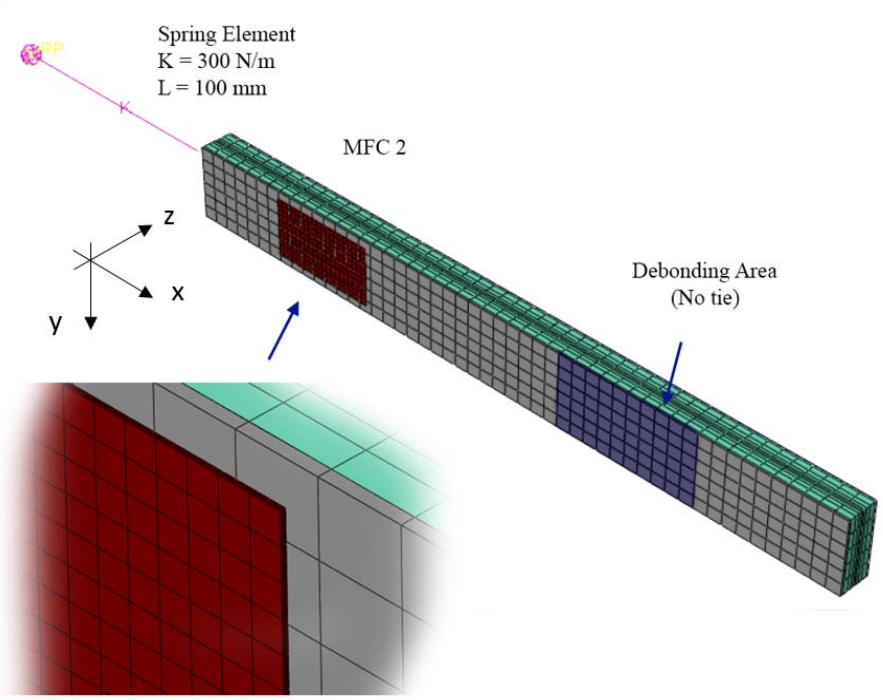

Figure 5: *Finite Element model for the sandwich structure – specimen S2E0P2.*

5 RESULTS

Vibration modes for the undamaged specimen and their respective non-damped natural frequencies obtained from preliminary FE analyses are shown in Figure 6 and Table 4.

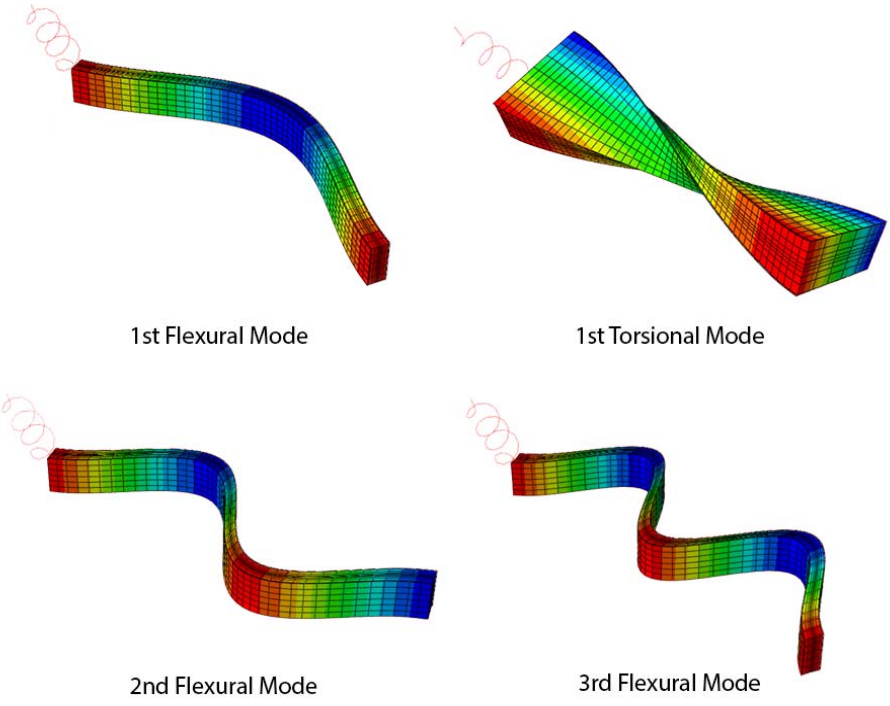

Figure 6: *Non-rigid modal shapes for the undamaged sandwich structure.*

Table 4: *Modal analysis – Numerical non-damped natural frequencies for specimen S1E0P0.*

Mode	Frequency [Hz]
1st Flexural	780.96
1st Torsion	932.15
2nd Flexural	1402.30
3rd Flexural	2042.00

After performing non-damped FE analyses, the experimental analyses were carried out at frequency range [0,4096] Hz. It is possible to verify that the highest frequency value selected for dynamic vibration tests is around the double of the value obtained via computational analyses. This strategy is used in order to guarantee the accuracy acquisition of the FRFs for the first natural frequencies and mode shapes. Table 5 shows natural frequencies and critical damping factors obtained experimentally for the six different types of specimens (damaged and undamaged, with and without MFC sensors). In general, as expected, the natural frequencies presented by the damaged structures are slightly lower than undamaged ones. Therefore, due to the presence of the debonding region, the stiffness of damaged structures is lower than undamaged ones. However, for flexural modes, this effect is very low, *i.e.* the debonding damage reduces a little the bending stiffness of sandwich structures. In addition, the natural frequencies increase with the inclusion of the MFC sensors. This is expected mainly for flexural modes due to the position of the smart patches. However, this increment is not so pronounced, because the density of PZTs sensors is much higher than the composites (see Tables 1 and 3).

Table 5: *Natural frequencies and critical damping factors obtained experimentally.*

Specimen:	S1E0P0		S1E0P1		S1E0P2	
	Frequency [Hz]	Damping Factor	Frequency [Hz]	Damping Factor	Frequency [Hz]	Damping Factor
	699.64	0.00798	704.42	0.00703	705.94	0.00760
	1343.91	0.01638	1338.62	0.01390	1348.84	0.01306
	2264.00	0.03083	2025.52	0.01396	2046.24	0.01185
Specimen:	**S2E0P0**		**S2E0P1**		**S2E0P2**	
	Frequency [Hz]	Damping Factor	Frequency [Hz]	Damping Factor	Frequency [Hz]	Damping Factor
	683.02	0.00730	689.59	0.00759	691.34	0.00799
	1317.94	0.01292	1309.59	0.01547	1325.12	0.01502
	1995.14	0.02161	1986.76	0.02366	1997.59	0.01484

Based on natural frequencies, as well as on mode shapes and critical damping factors, the frequency range of interest for the next analyses was set for three first flexural modes [50, 2300] Hz. In fact, due to the position of the MFC sensors, it was not possible to obtain the damping factors for torsion modes. Besides, it is important to highlight that critical damping factors for flexural modes obtained experimentally are used in the damped FE analyses to determine numerical FRFs.

5.1 Case Study 1: Influence of the MFC sensors

To verify the influence of the MFC sensors on the dynamic behavior of sandwich structure, FRF of the permanent accelerometer (Accelerometer 3) was compared to all specimens without damage. In other words, FRFs were obtained from specimens S1E0P0, S1E0P1 and S1E0P2. The results are shown in Figure 7 and Figure 8.

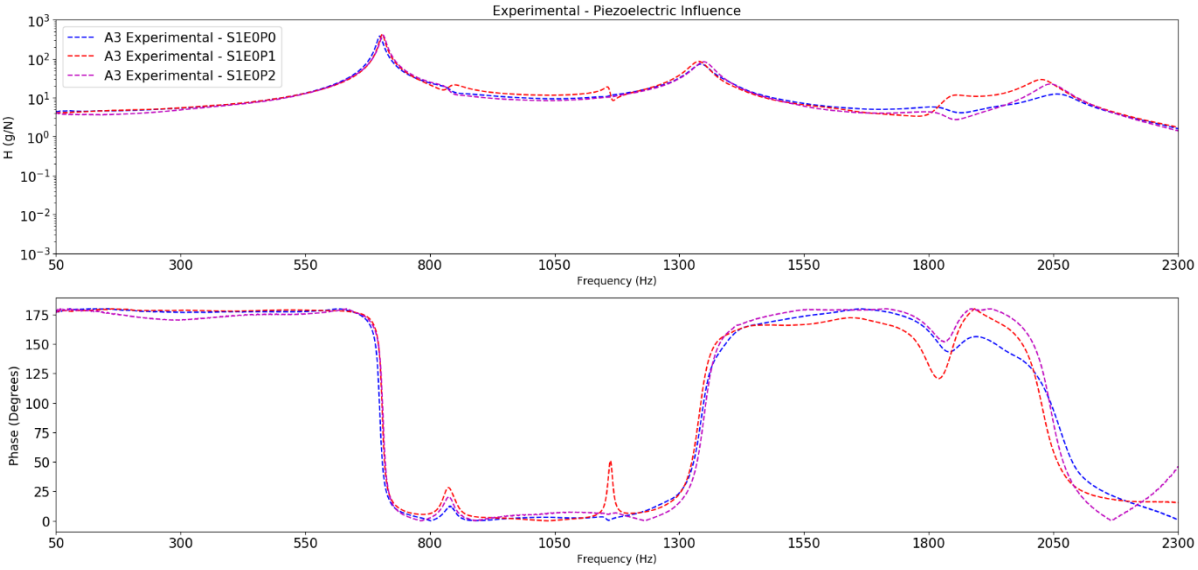

Figure 7: *Experimental results: Influence of the MFC sensors on the dynamic response – A3.*

By one hand, the influence of the MFC on the dynamic behavior of the sandwich structure is minimal as shown by the experimental results. On the other hand, the computational analyses showed much greater influence of the MFC sensors. This difference could be related to the model of the MFC sensors. In fact, this model depends on the distribution of the piezoelectric fibers in the sensor. This was not considered, because it was used a homogenized volume with density much higher than the composite material. Thus, probably, the mass of the FE model with MFC sensors is higher than without. It is clearly observed in the 3rd flexural mode (around 2050 Hz) shown by Figure 8.

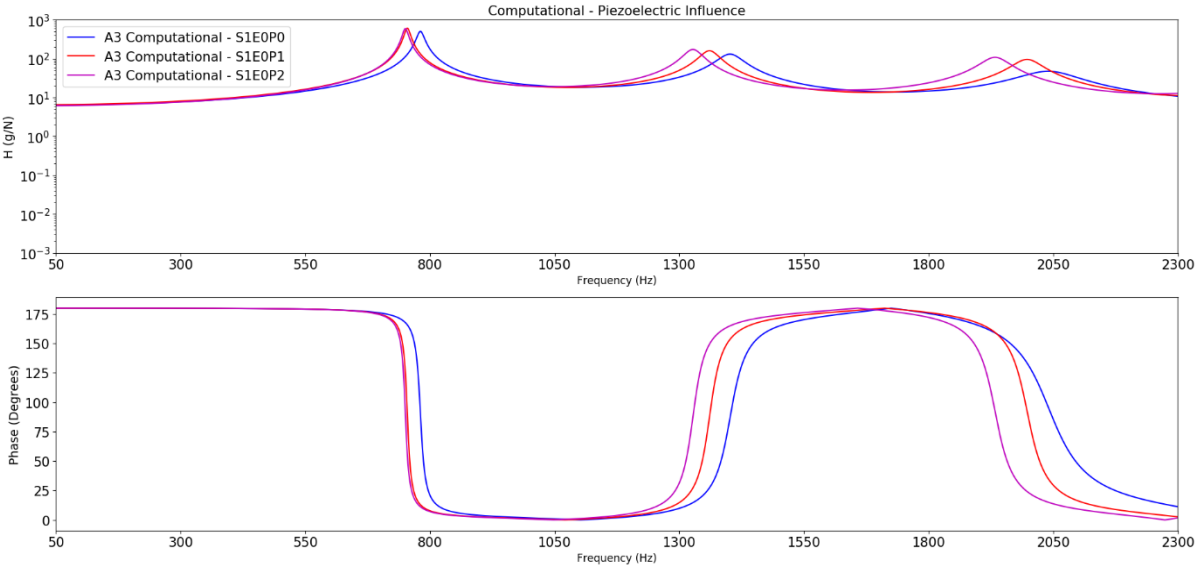

Figure 8: *Computational results: Influence of the MFC sensors on the dynamic response – A3.*

Comparing the experimental and computational responses of S1E0P0 in Figure 9, it becomes evident that the FE model displays higher stiffness values than experimental specimens. One possible explanation is the discrepancy between mechanical properties of the skins obtained from the literature and real properties for the specimens used.

In addition, FE analyses were carried out for a model with perfect mechanical properties and perfect adhesion between the skins and the core, whilst real specimens may present variations and imperfections introduced by the manufacturing and cutting process. By comparing the responses for specimen S1E0P2 (Figure 10) and S1E0P0 (Figure 9), it can be noticed that computational analysis also predicts higher influence of the MFC sensors than observed in experiments. However, in the Figue 10, computational model shows higher natural frequency value only for the first flexural mode, and lower values for the others when compared to experimental results. As commented from the results in Figure 8, the influence of the MFC sensors in the numerical simulation decreases the natural frequencies of the specimen due to the modelling approach, and the phenomenum is more accentuated in the second and third frequencies. It is also possible to confirm that the influence of the mass of the MFC sensor in the first mode is lower than the stiffness. In addition, it is very important to observe that damping effects have been considered in the FE analyses by using the damping factors measured experimentaly. However, other damping models can be applied in order to simulate better these effects.

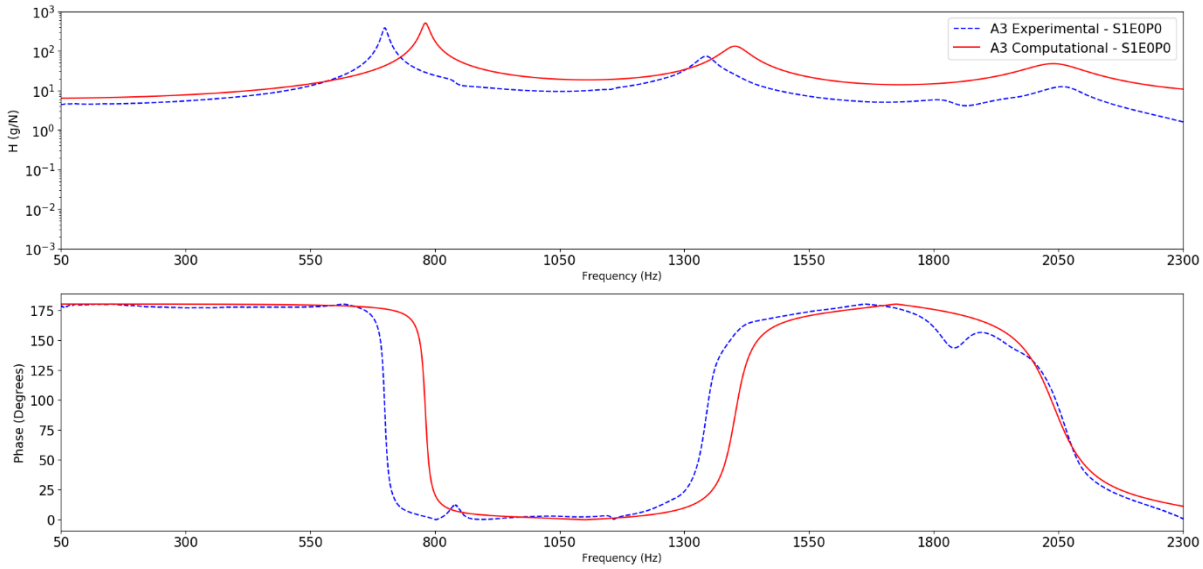

Figure 9: *Computational vs. Experimental results for S1E0P0.*

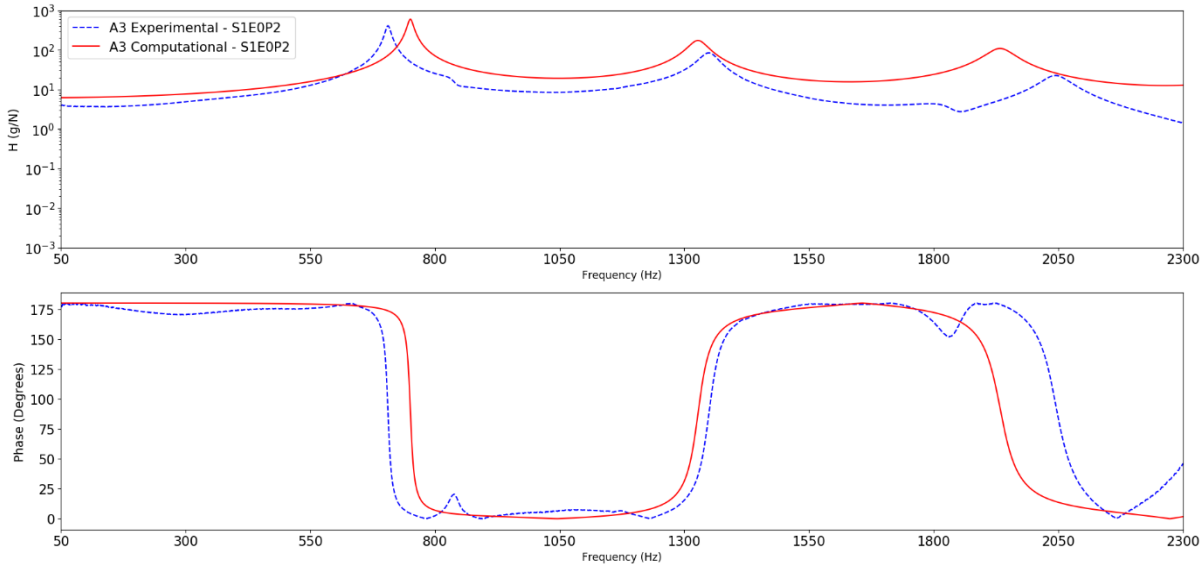

Figure 10: *Computational vs. Experimental results for S1E0P2.*

5.2 Case Study 2: Influence of the damage

The influence of the debonding damage was studied by comparing FRFs obtained from the accelerometers for the specimens without MFC sensors. The reason for this investigation is to isolate the influence of damage. Figure

11 shows the differences found in experimental FRFs. As shown by the preliminary analyses (see Table 5), the presence of the damage influences a little bit the behavior of the 1st flexural mode. It is possible to observe a little bit more influence on 2nd and 3rd flexural modes. As commented earlier, the effect of the debonding area on the flexural stiffness is very low.

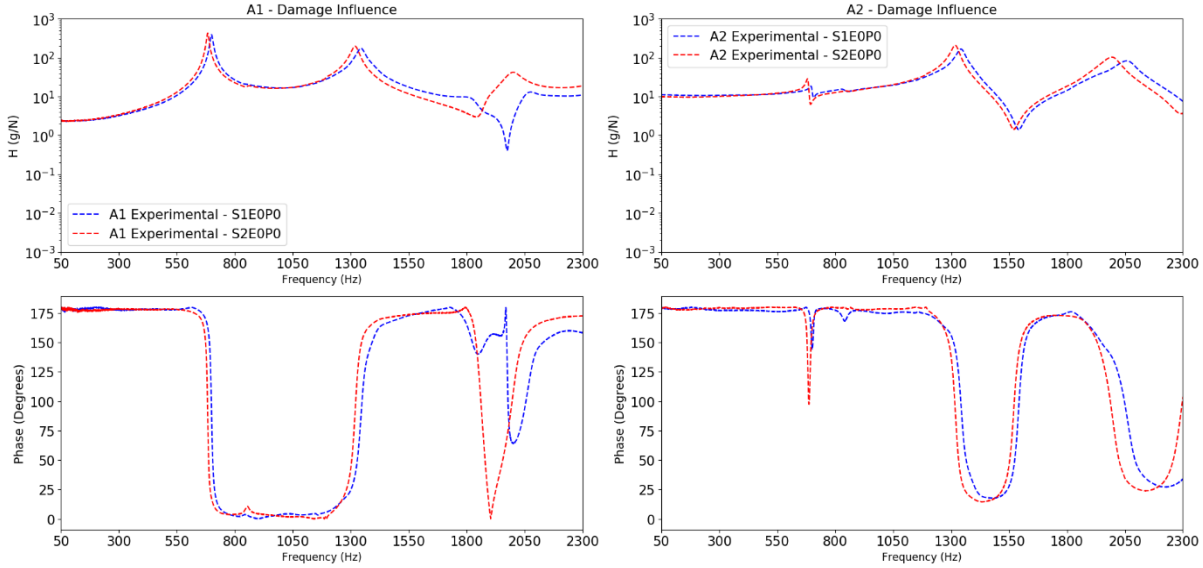

Figure 11: *Experimental results: Influence of debonding damage - A1 and A2.*

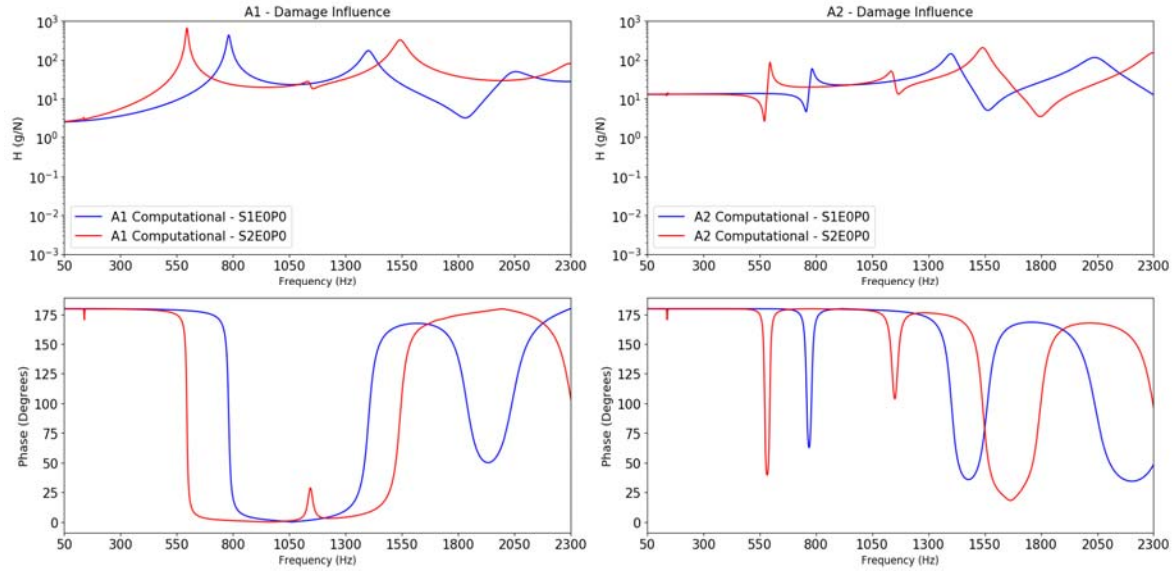

Figure 12: *Computational results: Influence of debonding damage - A1 and A2.*

On other hand, the influence of the debonding area in the computational analyses is in the opposite way. Observing the responses for accelerometer 1 and 2, the influence of damage in the FE model, as seen in Figure 12, is much more relevant compared to experimental results. One possible reason for this effect is the absence of contact models in the debonding area of computational analysis (steady state dynamic analysis), but friction and normal forces exist in real debonded area. Thus, in the experiments, this region might have resistance to movements due to the contact between the debonded surfaces. In addition, Figure 13 and Figure 14 show the experimental and computational results for accelerometer 3, and similar differences are confirmed.

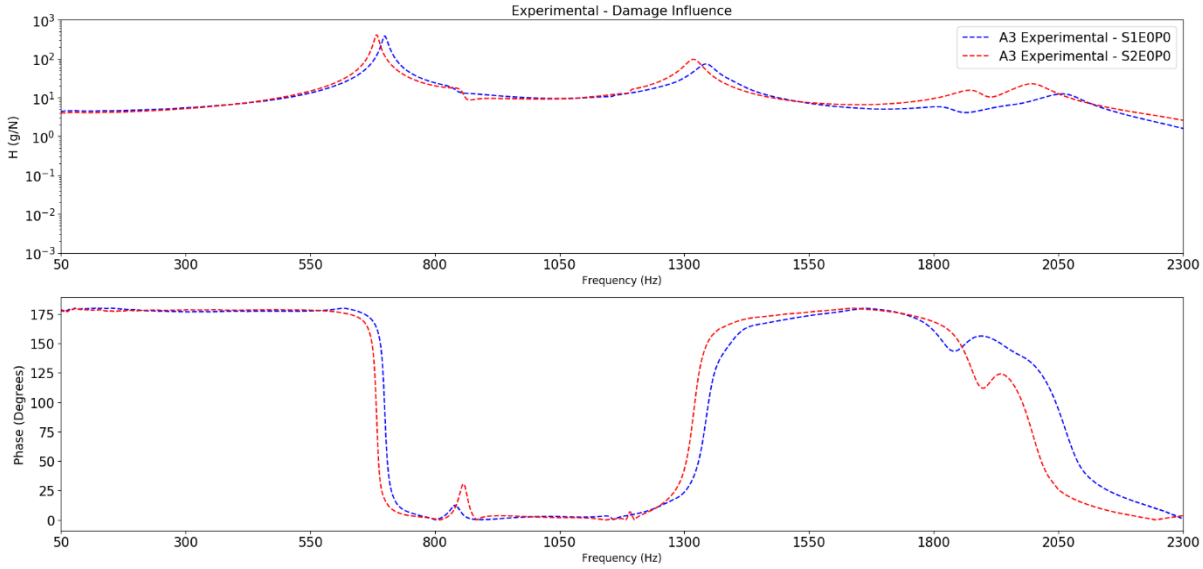

Figure 13: *Experimental results: Influence of debonding damage - A3.*

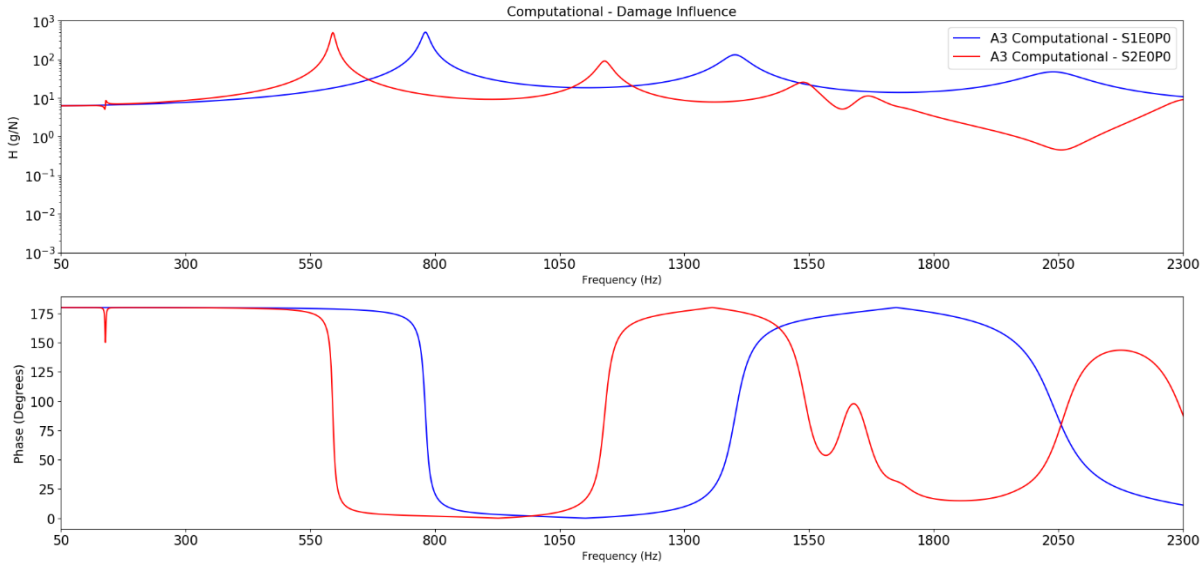

Figure 14: *Computational results: Influence of debonding damage - A3.*

5.3 Case Study 3: Damage identification

The damage identification is performed by two different MFC sensors, not by accelerometers. The purpose of this case study consists on using FRFs to observe the shift caused by the presence of damage, followed by damage metrics calculation. The Frequency Response Functions used for these analyses are shown in Figure 15 and Figure 16.

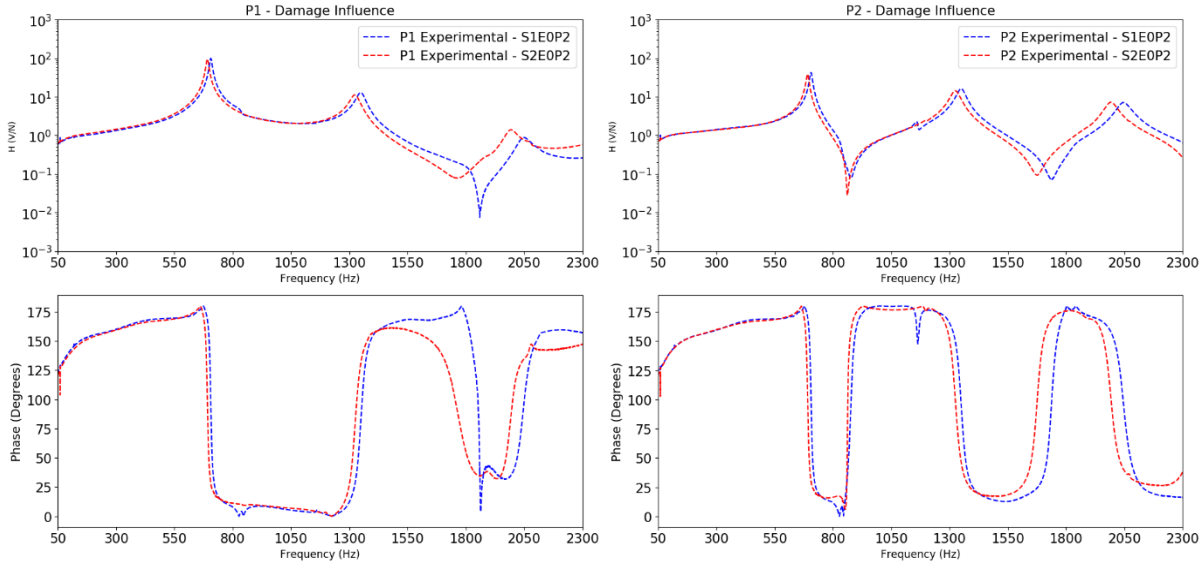

Figure 15: *Experimental results: Influence of the damage - P1 (MFC 1) and P2 (MFC 2).*

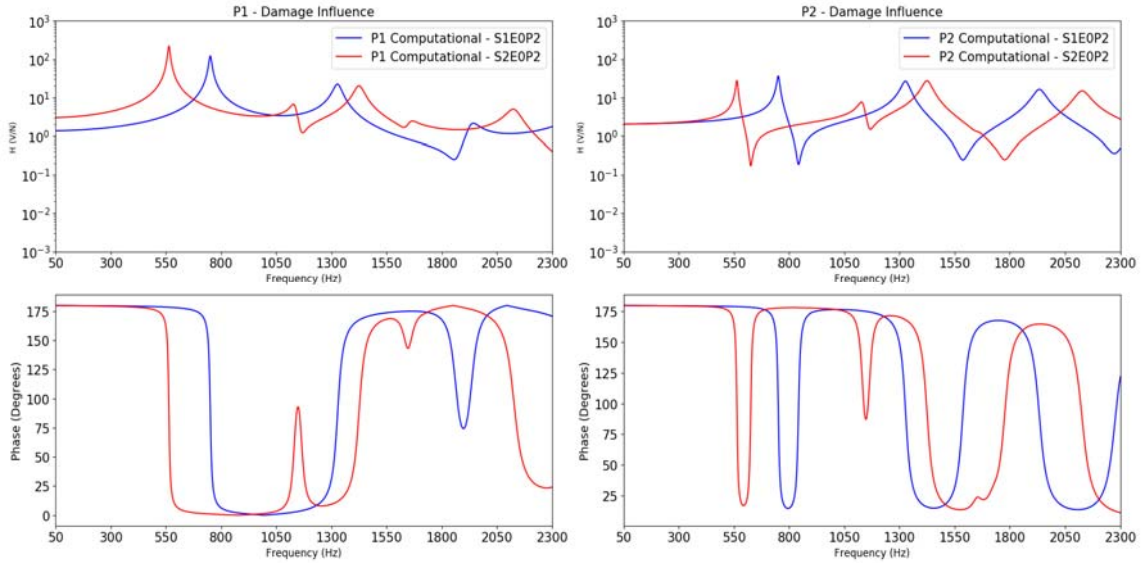

Figure 16: *Computational results: Influence of the damage - P1 (MFC 1) and P2 (MFC 2).*

As observed previously, computational analyses did not properly represent the damage in the structure due to the absence of contact models for simulating the debonded region. Therefore, the damage effect in the dynamic signature of the FE models is much greater than the experimental ones. In addition, there is the influence of the homogenization approach used to model the MFC sensors. Thus, it was not considered the distribution of piezoelectric fibers in the sensors.

Figure 17 shows the results for intact specimens (S1). The experimental and numerical dynamic signatures are slightly similar from MFC 2 (P2), where the highest differences are more evident for higher frequencies. It is important to highlight that there is a variation in the geometry of the specimens; in other words, there are average values with standard deviation for the dimensions of the sandwich beams. Therefore, in the simulations, it was used average values for the dimensions. This could explain the differences in all frequencies. On other hand, as shown by Figure 18, the experimental and numerical responses of the damaged specimens are not close even for lower frequencies from MFC 2 (P2). This could be explained based on different aspects, such as the material properties of skins obtained from literature used in the FE models and the absence of contact models to simulate the debonded region. In addition, there is a high difference for the perfect adhesion between skins and core simulated by the FE models and the glued real region, which may have imperfect adhesion due to manufacturing issues.

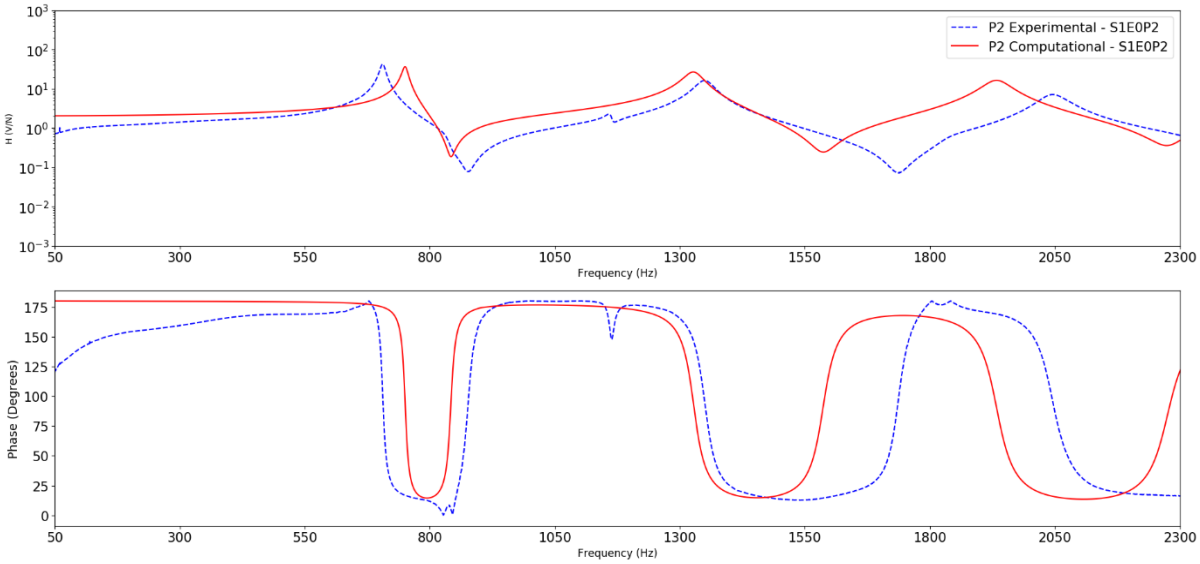

Figure 17: *Computational vs. Experimental results for S1E0P2 – P2 (MFC 2).*

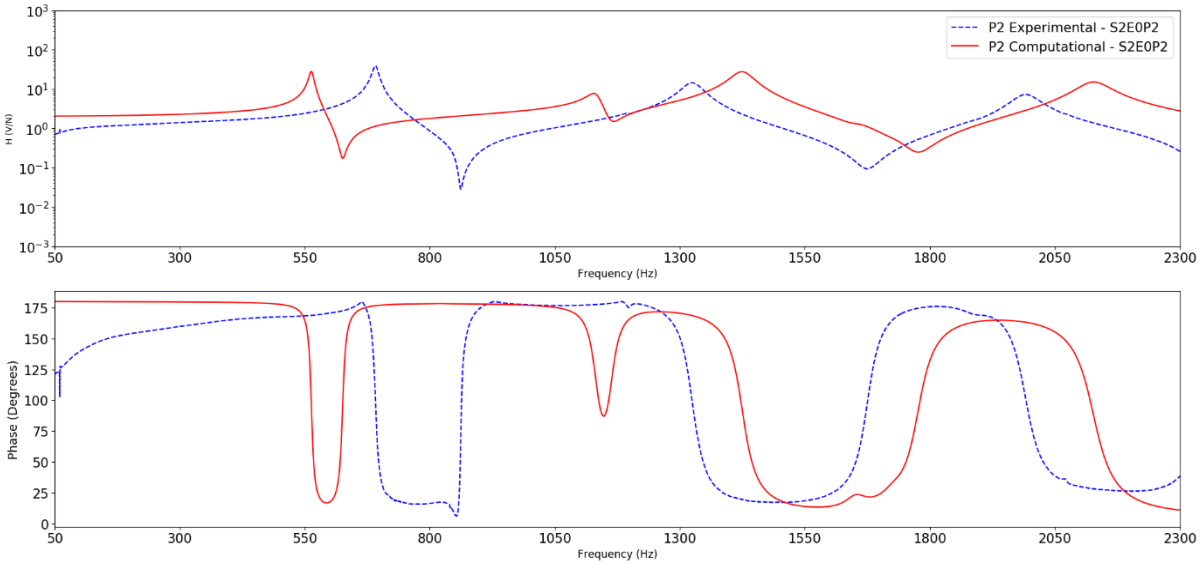

Figure 18: *Computational vs. Experimental results for S2E0P2 – P2 (MFC 2).*

Applying the damage metrics previously explained, it is possible to calculate damage indexes from FRFs of undamaged and damaged sandwich structures. The values are presented in Table 6 and Table 7. Considering Figure 1, H_{12} means input at position 1 and output at position 2 (from accelerometer 1 or MFC 1), H_{13} means input at position 1 and output at position 3 (from accelerometer 2 or MFC 2) and H_{15} means input at position 1 and output at position 5 (from permanent accelerometer 3).

Table 6: *Mickens' damage indexes (H is amplitude).*

	No MFCs		1 MFC		2 MFCs	
	DI (H)	DI (Phase)	DI (H)	DI (Phase)	DI (H)	DI (Phase)
FEA						
H_{12}	2.41	1.75	1.99	0.73	0.86	8.30
H_{13}	1.66	0.59	0.87	9.24	2.01	1.58
H_{15}	0.88	12.72	2.2	11.71	1.78	1.35
Experiments						
H_{12}	1.41	0.76	0.20	0.11	0.44	0.79
H_{13}	0.25	0.14	0.26	0.65	0.66	0.65
H_{15}	0.35	0.46	0.47	0.52	0.39	0.36

Table 7: *Damage indexes by using proposed procedure (H is amplitude).*

	No MFCs		1 MFC		2 MFCs	
	DI (H)	DI (Phase)	DI (H)	DI (Phase)	DI (H)	DI (Phase)
FEA						
H_{12}	0.27	0.25	0.31	0.24	0.30	0.41
H_{13}	0.34	0.25	0.31	0.46	0.26	0.27
H_{15}	0.30	0.47	0.25	0.32	0.32	0.34
Experiments						
H_{12}	0.12	0.10	0.09	0.08	0.08	0.10
H_{13}	0.10	0.11	0.08	0.10	0.06	0.11
H_{15}	0.09	0.09	0.07	0.12	0.10	0.11

Table 8: *Damage indexes for metrics I and II based on the amplitude of the FRF.*

	No MFCs		1 MFC		2 MFCs	
	DI Metric I	DI Metric II	DI Metric I	DI Metric II	DI Metric I	DI Metric II
FEA						
H_{12}	1.28	4.50e4	0.92	3.72e4	0.90	1.61e4
H_{13}	0.87	3.10e4	0.92	1.63e4	1.42	3.75e4
H_{15}	0.93	1.65e4	1.42	4.10e4	1.02	3.32e4
Experiments						
H_{12}	0.51	2.63e4	0.33	0.38e4	0.42	0.81e4
H_{13}	0.35	0.47e4	0.40	0.48e4	0.41	1.23e4
H_{15}	0.46	0.65e4	0.45	0.88e4	0.41	0.73e4

As evidenced by equations 3 and 6, the Mickens' damage index DI is a measure of the difference of the modal response between the undamaged and damaged condition, and returns a zero value if the difference is inexistent (meaning no damage in the specimen). Comparing Mickens' damage indexes (Table 6), it is possible to verify that the highest discrepancy is for experiments of H_{12}. It is verified that DI (Amplitude) obtained from accelerometer 1 is 1.41, and from MFC 1, it is 0.20 and 0.44 for one and two sensors present in the specimens, respectively.

For the damage metrics calculated by using the proposed procedure (Table 7), the DI (Amplitude) obtained by the MFC 1 for experiments of H_{12} is respectively 0.09 and 0.08, considering one and two sensors present in the specimens, respectively. And, the value obtained by the accelerometer for a specimen without MFC sensor is 0.12. The highest discrepancy observed in Table 7 is for FEA of H_{13}. It is verified that DI (Phase) obtained from MFC 2 is 0.46, considering one sensor present in the specimen. And, the accelerometer shows a damage index of 0.25.

In the same way that Mickens' Metric, Metrics I and II (equations 7 and 8) are also based on a comparison between the FRF of intact and damaged structure, and both return zero value when no damage is present. Table 8 presents the results for the damage indexes calculated via Metrics I and II based on the magnitudes of the FRF. The Damage Indexes calculated via Metric I are also very consistent, regardless of the sensoring method. For Metric II, however, these values are more spread. The damage index for experimental results of H_{12} using Metric II register a value of 2.63E4 when measured by accelerometer, and a value of 0.38E4 when measured by MFC 1 (with only one MFC present in the structure). It can be also seen that, regardless of the metric chosen, the damage indexes from the FEA are higher than those from the experimental analyses.

In summary, DI experimental values using the proposed procedure are satisfactory, in the sense that these results are less spread, showing more consistent values independently of the sensoring adopt (either using an accelerometer or MFC sensors). This is an important aspect because a reliable SHM system should be robust and steady. For computational analyses, however, the damage indexes are much greater than the experimental ones due to the different aspects, such as absence of contact models in the FE analyses, as well as material properties of the skins from literature, modeling approaches used to simulate MFC sensors and damping effects.

6 CONCLUSIONS

The usage of damage metrics showed to be imperative for damage identification in free-free sandwich structures. However, the damage metric proposed by Mickens showed some discrepancies between values, and the proposed procedure in the present work was able to reduce the dispersion between the results, while also preventing false positives that could appear from low number divisions in Mickens' damage index. A similar behavior was observed for damage indexes measured by Metric II, which displayed discrepant values of DI when using an accelerometer or a MFC. On the other hand, the results for Metric I exihibited more consistent values regardless of the sensoring adopt.

In addition, for the proposed procedure, the low dispersion in the results measured from accelerometers and MFC sensors demonstrated the viability of using smart materials such as the MFC in the health monitoring of these structures. This is important for the development of viable SHM systems, because MFCs offer high performance, reliability and simplicity to assemble and use ("plug and play") in a cost competitive device.

Regarding the FE models of the sandwich structures, debonding damage had stronger effect on the dynamic response compared to the experimental analyses. The discrepancy between the computational and the experimental results can be from problem during the manufacturing process to produce the damage (debonding area), so that there is an overestimation of the severity of damage in the finite element model compared to the real debonding extension in the structure. It is also difficult to control the process to glue the skin to the core of the sandwich structure, while the FE model assumes a perfect link between them. Another source of discrepancy can be due to differences in material properties of the skins used in the FE model and the real ones. In addition, the absence of contact models in the modal computational analysis (steady state dynamic analysis) promotes a more flexible structure than the real one, when there is a debonded region. Besides, modeling approaches used to simulate MFC sensors and damping effects could influence the numerical results. In fact, the computational analyses were used in this study mainly to provide a preliminary insight and the frequency range of interest for the experimental tests. They should be certainly improved for future studies, considering not only material properties from characterization tests for all elements (skins, MFC sensor and core, including viscoelastic properties), but also the application of other finite element formulations.

Finally, an important conclusion is that the proposed method based on FRFs (amplitude and phase) can be used to detect damage in composite structures. In other words, there is a good prospect for the application of this method and MFC sensors in SHM systems for composite sandwich structures.

Acknowledgements

The authors are thankful for the support of the National Council of Scientific and Technological Development (CNPq process number: 139806/2013-0, 152445/2016-1, 401170/2014-4 and 310094/2015-1) for funding this research. Volnei Tita would like to thank the financial support of the Air Force Office of Scientific Research – AFOSR (Grant FA9550-16-1-0222) and Sao Paulo Research Foundation (FAPESP).

References

Amir, S., Morlier, J., Gourinat, Y, (2010), "Damage monitoring in sandwich beams by modal parameter shifts: A comparative study of burst random and sine dwell vibration testing", Journal of Sound and Vibration, v. 329, no. 5, p. 566-584.

Caliri Junior, M. F., Soares, G. P., Angelico, R. A., Canto, R. B., Tita, V., (2012), "Study of an Anisotropic Polymeric Cellular Material Under Compression Loading", Materials Research, 15(3), pp 359 – 364.

Callister, W. D.; Rethwisch, D. G., (2012), "Fundamentals of Materials Science and Engineering: An Integrated Approach", John Wiley & Sons, Inc. 4th Edition.

Dhamande, L. S., Bhaskar, R. V., (2014), "Damage Detection in Aluminium Honeycomb Structure using Vibration Analysis", International Journal of Current Engineering and Technology, v.5 n.5.

Doebling, S.W.; Farrar, C.R.; Prime, M.B.; Shevitz, D.W., (1996), Damage identification and health monitoring of structural and mechanical systems from changes in their vibration characteristics: A literature review, page 2, Technical report, Los Alamos National Laboratory Report LA-13070-MS, Los Alamos, New Mexico.

Flor, F. R. (2015) "Damage monitoring in composite structures via vibration based method: metal-composite bonded joints and sandwich structures." Master Thesis, University of São Paulo, Brazil.

Idriss, M.; Mahi, A. E.; Guerjouma, R. E.; (2015), "Characterization of Sandwich Beams With Debonding by Linear and Nonlinear Vibration Method", Composite Structures, v.120, p.200-207.

Leijten, J.; Bersee, H. E. N.; Bergsma, O. K.; Beukers, A.; (2009), "Experimental study of the low-velocity impact behaviour of primary sandwich structures in aircraft", Composites: Part A, v.40, p. 164-175.

Lestari, W., Qiao, P., (2005), "Damage detection of fiber-reinforced polymer honeycomb sandwich beams", Composite Structures, v. 67, n. 3, p. 365-373.

Li, B.; Li, Z.; Zhou, J.; Ye, L.; Li, E.; (2015), "Damage Localization in Composite Lattice Truss Core Sandwich Structures Based on Vibration Characteristics", Composite Structures, v.126, p.34-51.

Luchinsky, D. G.; Hafiychuk, V.; Smelyanskiy, V.; Tyson, R. W.; Walker, J. L.; Miller, J. L.; (2011), "High-fidelity modeling for health monitoring in honeycomb sandwich structures", In: Aerospace Conference, IEEE. p. 1-7.

Medeiros, R. (2016) "Development of a criterion for predicting residual strength of composite structures damaged by impact loading." Ph.D. Thesis, University of São Paulo, Brazil.

Medeiros, R.; Vandepitte, D.; Tita, V. (2017), "Structural health monitoring for impact damaged composite: a new methodology based on a combination of techniques". Structural Health Monitoring, v. online, p. 147592171668844 (DOI: 10.1177/1475921716688442).

Mickens, T., Schulz, M., Sundaresan, M., Ghoshal, A., Naser, A. And Reichmeider, R., (2003), "Structural health monitoring of an aircraft joint", Mechanical Systems and Signal Processing, v. 17, No. 2, pp. 285 – 303.

Mustapha, S.; Ye, L.; Dong, X.; Alamdari, M. M., (2016), "Evaluation of Barely visible indentation damage (BVID) in CF/EP Sandwich Composites Using Guided Wave Signals", Mechanical Systems and Signal Processing, v.76-77, p.497-517.

Nguyen, M. Q.; Jacombs, S. S.; Thomson, R. S.; Hachenberg, D.; Scott, M. L.; (2005), "Simulation of impact on sandwich structures", Composite Structures, v. 67, p. 217-227.

Oruganti, K., M. Mehdizadeh, S. John, And I. Herszberg., (2009), "Vibration-based Analysis of Damage in Composites". In The 2nd Asia-Pacific Workshop on Structural Health Monitoring (2APWSHM), edited by S. Galea, W. Chiu, and A. Mita. Institute of Materials Engineering.

Pourmoayed, A. R.; Malekzadeh Fard, K.; Shahravi, M., (2017), "Vibration Analysis of a Cylindrical Sandwich Panel with Flexible Core Using an Improved Higher-Order Theory", Latin American Journal of Solids and Structures, v.14, p.714-742.

Sartorato, M., Medeiros, R., Tita, V., (2015), "A finite element formulation for smart piezoelectric composite shells: Mathematical formulation, computational analysis and experimental evaluation", Composite Structures, v. 127, p. 185-198.

Sartorato, M., Medeiros, R., Vandepitte, D., Tita, V., (2017), "Computational model for supporting SHM systems design: Damage identification via numerical analyses", Mechanical Systems and Signal Processing, v. 84, p. 445-461.

Singh, C.V. And Talreja, R., (2010), "Evolution of ply cracks in multidirectional composite laminates", International Journal of solids and structures, v. 47. pp. 1338-1349.

Tita, V., Caliri Junior, M. F., (2012), "Numerical Simulation of Anisotropic Polymeric Foams", Latin American Journal of Solids and Structures, pp 1 -21.

Tita, V., Caliri Junior, M. F., Angelico, R. A., Canto, R. B., (2012), "Experimental Analyses of the Poly(vinyl chloride) Foams' Mechanical Anisotropic Behavior", Polymer Engineering and Science, v. 52, pp. 2654-2663

Yam, L. H.; Yan, Y. J.; Jiang, J. S.; (2003), "Vibration-based damage detection for composite structures using wavelet transform and neural network identification", Composite Structures, v. 60, p. 403-412.